European Heart Journal (2020) **0**, 1–13
doi:10.1093/eurheartj/ehaa140

ESC European Society of Cardiology

**BASIC SCIENCE**
*Lipids*

# The haemochromatosis gene Hfe and Kupffer cells control LDL cholesterol homeostasis and impact on atherosclerosis development

**Egon Demetz[1], Piotr Tymoszuk [1], Richard Hilbe[1], Chiara Volani [1], David Haschka [1], Christiane Heim[1], Kristina Auer[1], Daniela Lener [2], Lucas B. Zeiger [1], Christa Pfeifhofer-Obermair [1], Anna Boehm [1], Gerald J. Obermair [3,4], Cornelia Ablinger [3], Stefan Coassin [5], Claudia Lamina[5], Juliane Kager[1], Verena Petzer [1], Malte Asshoff[1], Andrea Schroll [1], Manfred Nairz [1], Stefanie Dichtl [1], Markus Seifert[1,6], Laura von Raffay[1], Christine Fischer[1], Marina Barros-Pinkelnig[1], Natascha Brigo [1], Lara Valente de Souza [1,6], Sieghart Sopper [7], Jakob Hirsch [8], Michael Graber [8], Can Gollmann-Tepeköylü [8], Johannes Holfeld [8], Julia Halper [1], Sophie Macheiner [9], Johanna Gostner [10], Georg F. Vogel[11], Raimund Pechlaner [12], Patrizia Moser[13], Medea Imboden [14,15], Pedro Marques-Vidal [16], Nicole M. Probst-Hensch[14,15], Heike Meiselbach[17], Konstantin Strauch[18,19], Annette Peters[20,21,22], Bernhard Paulweber [23], Johann Willeit [12], Stefan Kiechl [12], Florian Kronenberg [5], Igor Theurl [1], Ivan Tancevski [1]*, and Guenter Weiss [1,6]***

[1]Department of Internal Medicine II, Medical University of Innsbruck, Anichstraße 35, 6020 Innsbruck, Austria; [2]Department of Internal Medicine III, Medical University of Innsbruck, Anichstraße 35, 6020 Innsbruck, Austria; [3]Department of Physiology and Medical Physics, Medical University of Innsbruck, Fritz-Pregl-Straße 3, 6020 Innsbruck, Austria; [4]Division of Physiology, Karl Landsteiner University of Health Sciences, Dr.-Karl-Dorrek-Straße 30, 3500 Krems, Austria; [5]Department of Genetics and Pharmacology, Institute of Genetic Epidemiology, Medical University of Innsbruck, Schöpfstraße 41, 6020 Innsbruck, Austria; [6]Christian Doppler Laboratory for Iron Metabolism and Anemia Research, Medical University of Innsbruck, Innsbruck, Austria; [7]Department of Internal Medicine V, Medical University of Innsbruck, Anichstraße 35, 6020 Innsbruck, Austria; [8]Department of Cardiac Surgery, Medical University of Innsbruck, Anichstraße 35, 6020 Innsbruck, Austria; [9]Department of Internal Medicine I, Medical University of Innsbruck, Anichstraße 35, 6020 Innsbruck, Austria; [10]Division of Medical Biochemistry, Medical University of Innsbruck, Innrain 80/IV, 6020 Innsbruck, Austria; [11]Department of Pediatrics I, Medical University of Innsbruck, Anichstraße 35, 6020 Innsbruck, Austria; [12]Department of Neurology, Medical University of Innsbruck, Anichstraße 35, 6020 Innsbruck, Austria; [13]Department of Pathology, Innsbruck University Hospital, Anichstraße 35, 6020 Innsbruck, Austria; [14]Swiss Tropical and Public Health Institute, Socinstraße 57, 4051 Basel, Switzerland; [15]Department of Public Health, University of Basel, Bernoullistraße 28, 4056 Basel, Switzerland; [16]Department of Internal Medicine, Lausanne University Hospital, Rue du Bugnon 46, 1011 Lausanne, Switzerland; [17]Department of Nephrology and Hypertension, University Hospital Erlangen, Maximiliansplatz 2, 91054 Erlangen, Germany; [18]Institute of Genetic Epidemiology, Helmholtz Zentrum München—German Research Center for Environmental Health, Ingolstädter Landstraße 1, 85764 Neuherberg, Germany; [19]Institute of Medical Informatics, Biometry and Epidemiology, Ludwig-Maximilians-Universität, Marchioninistraße 15, 81377 Munich, Germany; [20]Institute of Epidemiology II, Helmholtz Zentrum München—German Research Center for Environmental Health, Ingolstädter Landstraße 1, 85764 Neuherberg, Germany; [21]German Center for Diabetes Research, Ingolstädter Landstraße 1, 85764 Neuherberg, Germany; [22]German Center for Cardiovascular Research, Lazarettstraße 36, 80636 Munich, Germany; and [23]First Department of Medicine, Paracelsus Medical University Salzburg, Strubergasse 21, 5020 Salzburg, Austria

*Received 21 July 2019; revised 16 October 2019; editorial decision 14 February 2020; accepted 18 February 2020*

**Aims** Imbalances of iron metabolism have been linked to the development of atherosclerosis. However, subjects with hereditary haemochromatosis have a lower prevalence of cardiovascular disease. The aim of our study was to understand the underlying mechanisms by combining data from genome-wide association study analyses in humans, CRISPR/Cas9 genome editing, and loss-of-function studies in mice.

* Corresponding authors. Tel: +43 512 504 23251, Email: Guenter.Weiss@i-med.ac.at (G.W.); Tel: +43 512 504 23251, Email: Ivan.Tancevski@i-med.ac.at (I.T.)

**Methods and results** Our analysis of the Global Lipids Genetics Consortium (GLGC) dataset revealed that single nucleotide polymorphisms (SNPs) in the haemochromatosis gene *HFE* associate with reduced low-density lipoprotein cholesterol (LDL-C) in human plasma. The LDL-C lowering effect could be phenocopied in dyslipidaemic *ApoE*$^{-/-}$ mice lacking *Hfe*, which translated into reduced atherosclerosis burden. Mechanistically, we identified HFE as a negative regulator of LDL receptor expression in hepatocytes. Moreover, we uncovered liver-resident Kupffer cells (KCs) as central players in cholesterol homeostasis as they were found to acquire and transfer LDL-derived cholesterol to hepatocytes in an Abca1-dependent fashion, which is controlled by iron availability.

**Conclusion** Our results disentangle novel regulatory interactions between iron metabolism, KC biology and cholesterol homeostasis which are promising targets for treating dyslipidaemia but also provide a mechanistic explanation for reduced cardiovascular morbidity in subjects with haemochromatosis.

**Keywords** Haemochromatosis • Atherosclerosis • LDL receptor • Kupffer cells • ABCA1



## Translational perspective

Dyshomeostasis of iron metabolism has been linked to the development of cardiovascular disease. By mining data of genome-wide association studies, we show that *HFE* variants associate with plasma low-density lipoprotein cholesterol (LDL-C) in humans, which was corroborated in a meta-analysis comprising six epidemiological studies ($n = 24\ 058$) where individuals carrying non-functional *HFE* displayed significantly reduced plasma LDL-C levels. Accordingly, *ApoE*$^{-/-}$ mice lacking *Hfe* in a setting of dietary iron overload display reduced plasma LDL-C levels, translating into inhibition of atherosclerosis. We identify HFE as a negative regulator of LDL receptor expression in hepatocytes, while iron overload triggers both the uptake and subsequent Abca1-dependent transflux of cholesterol from Kupffer cells (KCs) to hepatocytes. Our data on the interaction between HFE, iron, KC, and LDL-C homeostasis may pave the way for the development of novel therapeutic strategies to combat cardiovascular disease in humans.

# Introduction

Hypercholesterolaemia is a major risk factor for atherosclerosis, and reduction of low-density lipoprotein cholesterol (LDL-C) has been shown to protect from the development of cardiovascular disease.[1] As current therapeutics do not always achieve this goal new therapeutic approaches to treat hypercholesterolaemia are needed.[2,3]

Iron overload has been linked to an increased risk for atherosclerosis. However, current epidemiologic and experimental evidence is not consistent.[4,5] A well-studied cause for parenchymal iron overload is hereditary haemochromatosis (HH) mostly being the consequence of a missense mutation of the gene *HFE* (C282Y), resulting in dysfunctional HFE retained in the endoplasmic reticulum,[6] instead of being transported to the plasma membrane. Hereditary haemochromatosis represents one of the most frequent autosomal recessive genetic disorders in people of Northern and Western European ancestry with a C282Y (rs1800562) heterozygote frequency between 1:10 and 1:15.[7,8] Thereby, HH subjects develop progressive parenchymal iron overload in parenchymal organs such as liver, pancreas, endocrine organs, and heart resulting in potential organ failure over time.[7,9] Surprisingly, a recent study with 2890 European C282Y homozygous HH patients revealed a significantly reduced risk for cardiovascular disease compared to age-matched subjects.[10] In line, both total cholesterol and LDL-C plasma levels were reduced in C282Y homozygotes compared to HFE wild-type study participants.[11] In contrast, a previous report found an increased risk for acute myocardial infarction in heterozygous patients carrying a C282Y mutation,[12] a group which is very unlikely to have significant iron overload.[11] Thus, further studies are urgently needed to disentangle the functional and clinical association between LDL-C levels, iron homeostasis, HFE alleles, and atherosclerosis development.

The liver is central for the control of iron homeostasis[13] but also pivotal for cholesterol metabolism.[14] Thus, a physiological interplay between iron and cholesterol metabolism could be hypothesized. The liver is composed of numerous different cell types including parenchymal hepatocytes, but also resident myeloid cells, called Kupffer cells (KCs).[15] Due to their micro-anatomical proximity, KCs appear to interact with hepatocytes in a paracrine manner.[16] Kupffer cells critically contribute to clearance of aged erythrocytes and thus to maintenance of iron homeostasis in the body.[17] So far, neither a role of iron on lipid homeostasis nor an impact of KCs on hepatocyte and whole-body cholesterol homeostasis has been systematically investigated.

Here, we uncover novel functions of KCs, iron, and hepatocyte HFE in the regulation of cholesterol homeostasis. We identify HFE as an important regulator of hepatocyte LDL receptor (LDLr) functionality and show that KCs contribute to LDL-C plasma clearance, which is affected by body iron levels. Our data identify novel physiological mechanisms with importance for cardiovascular diseases but also recommend KCs and HFE as novel therapeutic targets to prevent atherosclerosis.

# Methods

*ApoE*$^{-/-}$*Hfe*$^{-/-}$ mice on C57BL/6N background were fed a western-type diet supplemented with 25 g/kg (iron$^{hi}$) or 5 mg/kg carbonyl iron (iron$^{lo}$), respectively. Genome-wide association studies (GWASs) on *HFE* were performed using the Global Lipids Genetics Consortium (GLGC) dataset

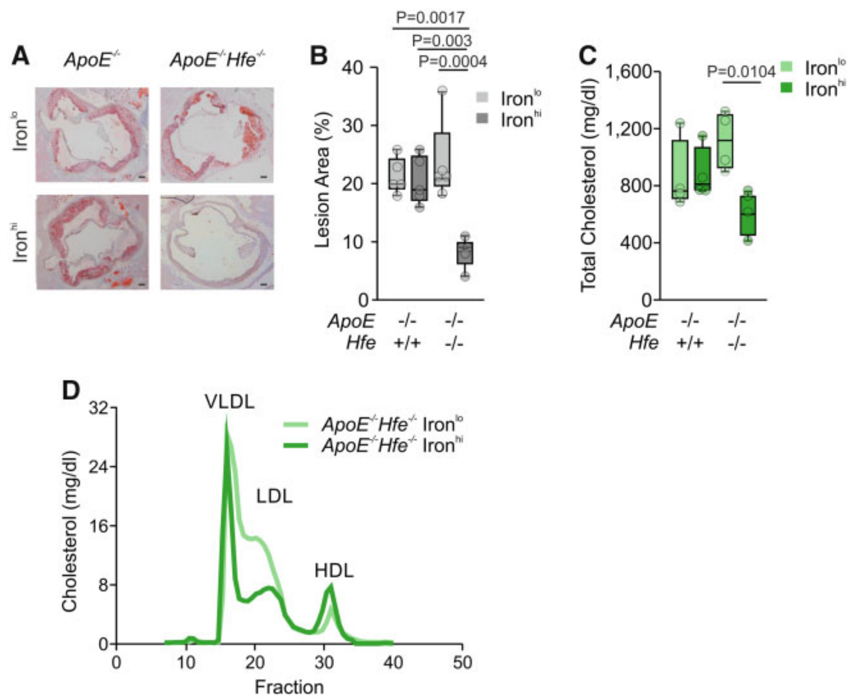


**Figure 1** Dietary iron supplementation reduces atherosclerosis development in *ApoE*$^{-/-}$*Hfe*$^{-/-}$ mice. *ApoE*$^{-/-}$*Hfe*$^{-/-}$ mice were fed a western-type diet with low or high iron content (iron$^{lo}$, iron$^{hi}$) for 20 weeks. (*A*) The atherosclerotic burden was visualized in aortic sections stained with Oil-Red-O (*n* = 5 per group). Scale bar = 100 µm. (*B*) Statistical comparison of the atherosclerotic lesion size of the aortic roots, respectively (*n* = 5 per group). (*C*) Plasma total cholesterol levels in *ApoE*$^{-/-}$ and *ApoE*$^{-/-}$*Hfe*$^{-/-}$ mice (*n* = 4 per group). (*D*) Fast protein liquid chromatography analysis of plasma pooled from *ApoE*$^{-/-}$*Hfe*$^{-/-}$ mice upon 10 weeks of diet (*n* = 4 per group).

(*n* = 196 475) and confirmed in further 24 058 individuals using a recessive model. Detailed methods and statistics are included in the Supplementary material online.

# Results

## High iron diet decreases atherosclerosis formation in *Hfe*-deficient mice

To elucidate whether HFE and/or systemic iron levels would affect cholesterol metabolism and atherosclerosis development, we cross-bred dyslipidaemic *ApoE*$^{-/-}$ mice with *Hfe*$^{-/-}$ animals and fed both *ApoE*$^{-/-}$, and *ApoE*$^{-/-}$*Hfe*$^{-/-}$ mice a western-type diet, either high in iron (iron$^{hi}$, 25 g/kg carbonyl-iron), or low in iron content (iron$^{lo}$, 5 mg/kg carbonyl-iron) for 20 weeks. Surprisingly, the iron$^{hi}$ diet led to a highly significant (>70%) reduction of atherosclerotic plaque formation in *ApoE*$^{-/-}$*Hfe*$^{-/-}$ animals, while *ApoE*$^{-/-}$ on the same diet did not benefit from iron supplementation (*Figure 1A* and *B*, and Supplementary material online, *Figure S1A–H*). Remarkably, and in accordance with the iron distribution pattern in Hfe related haemochromatosis, iron was stored in hepatic parenchymal cells[7–9] of *Hfe*$^{-/-}$ mice on an iron rich diet but did neither accumulate in resident macrophages including hepatic KCs nor in foam cells within the atherosclerotic lesion (Supplementary material online, *Figure S2A–H*). Importantly, iron supplementation was not associated with reduced plaque stability as compared to mice receiving a low iron diet (Supplementary material online, *Figure S3A–D*).

In line with the atherosclerotic burden, no reduction in plasma cholesterol levels was observed in *ApoE*$^{-/-}$ knockouts fed the iron$^{hi}$ diet, whereas iron$^{hi}$ diet led to a significant decrease in plasma cholesterol levels of *ApoE*$^{-/-}$*Hfe*$^{-/-}$ mice (*Figure 1C*). Lipoprotein separation analysis via fast protein liquid chromatography revealed a clear reduction of the LDL-C fraction in mice with HFE deficiency and fed an iron-rich diet over time (*Figure 1D*, Supplementary material online, *Figure S4*), while no such changes were observed in wild-type mice receiving diets with different iron contents (Supplementary material online, *Figure S5*). Of note, iron supplementation decreased the amount of ApoB-containing lipoproteins, regardless of the amount of cholesterol in the diet (Supplementary material online, *Figure S6A and B*).

Thus, our results suggest a gene effect for *Hfe* on cholesterol homeostasis upon iron supplementation. Crucially, a cholesterol-lowering effect of Hfe deficiency was already detectable after 5 days of exposure of mice to either iron$^{hi}$ or iron$^{lo}$ diets (Supplementary material online, *Figure S7A and B*). Importantly, feeding an iron$^{hi}$ diet for 10 weeks did not result in increased concentrations of circulating inflammatory cytokines in serum in *ApoE*$^{-/-}$*Hfe*$^{-/-}$ mice, neither did it modulate the numbers of circulating monocytes or macrophages, nor the expression of inflammatory markers on their surface, liver function tests, or the expression of M1/M2 type macrophage-specific gene signatures within the plaque when compared with mice receiving an iron-deficient diet (Supplementary material online, *Figure S8A–H*), corroborating data obtained from whole-blood transcriptome of healthy and HH type 1 individuals[18,19] (Supplementary material online, *Figure S9A–C*).

Of note, foam cell staining was even reduced within the plaques of $ApoE^{-/-}Hfe^{-/-}$ mice on $iron^{hi}$ diet as compared to mice receiving a low iron diet (Supplementary material online, *Figure S2D and F*). In line, the expression of hallmark genes for regulatory T cells (Treg), Th2 and Th1 cells were found to be reduced in atherosclerotic lesions of $iron^{hi}$ animals as compared to $iron^{lo}$ mice (Supplementary material online, *Figure S10A–G*). Interestingly, reduced foam cell numbers together with dampened T-cell activation was not associated with altered plaque composition in terms of collagen and muscle fibre content when comparing $ApoE^{-/-}Hfe^{-/-}$ mice receiving either $iron^{hi}$ or $iron^{lo}$ diets (Supplementary material online, *Figure S3A–C*).

## Identification of HFE as a regulator of low-density lipoprotein cholesterol

We mined the data from a published GWAS (*n* > 188 000) for significant association signals in and close to the HFE gene (±10 kbp).[20] The rs1800562 polymorphism showed a significant association with plasma LDL cholesterol (*Figure 2A*) but not with high-density lipoprotein cholesterol (HDL-C) (Supplementary material online, *Figure S11A and B*) suggesting a link of HFE expression to LDL-C levels (Supplementary material online, *Figure S12A*). Importantly, the allele of rs1800562 causes the C282Y mutation of the HFE gene, which leads to HH.[6,9] We therefore performed a recessive model for rs1800562 on total cholesterol as well as LDL-C in 6 epidemiological studies (Supplementary material online, *Table S1* and *Figure S12B*). We found a significant reduction of total cholesterol (-19.50 mg/dL, $P = 0.0004$; Supplementary material online, *Figure S12C*), and LDL-C (-15.25 mg/dL, $P = 0.001$; *Figure 2B*) in individuals carrying the homozygous minor allele genotype (AA) compared to GG/AG genotypes. In summary, GWAS and association analyses in humans strongly support the relationship between HFE and LDL-C observed in a mouse model of haemochromatosis.

In addition, we measured plasma HDL-C (Supplementary material online, *Figure S13A*), and plasma ApoA-I (Supplementary material online, *Figure S13B*) in $ApoE^{-/-}Hfe^{-/-}$ animals set on $iron^{hi/lo}$ diet for 10 weeks. Hyperferric animals showed increased levels of HDL-C but no changes in plasma ApoA-I as compared to mice receiving a $iron^{lo}$ diet. To test whether increased HDL-C content without changes in ApoA-I translates into increased HDL function, we performed macrophage-to-feces reverse cholesterol transport (RCT) studies in $ApoE^{-/-}Hfe^{-/-}$ set on $iron^{hi/lo}$ diet for 3 weeks. After intraperitoneal injection of [$^3$H]-cholesterol-labelled J774 macrophages, we detected no significant differences in plasma tracer levels over time (Supplementary material online, *Figure S13C*); as well as we did not observe any changes in faecal [$^3$H]-sterol levels (Supplementary material online, *Figure S13D*), respectively. Taken together, $iron^{hi}$ diet did increase plasma HDL-C levels but not the functionality of HDL particles in terms of RCT.

## Genetic reconstitution of HFE in *Hfe*$^{-/-}$ hepatocytes dramatically reduces low-density lipoprotein receptor expression

To understand the mechanisms underlying the associations between the *HFE* C282Y variant and LDL-C in humans and mice we created expression plasmids encoding either wild-type (*pCS2-HA-HFE(282C)*) or missense (*pCS2-HA-HFE(282Y)) HFE* for reconstitution experiments in primary hepatocytes derived from $Hfe^{-/-}$ mice. As shown in *Figure 3A–C*, primary murine $Hfe^{-/-}$ hepatocytes reconstituted with wild-type *HFE* displayed a marked reduction in the expression of the LDLr compared to non-transfected cells (arrow), and compared to hepatocytes reconstituted with the *HFE* C282Y variant (*Figure 3D and F*, integrated grey scale quantification in *Figure 3G*). These experiments demonstrate that HFE is a negative regulator of LDLr expression and suggest that the identified lead SNP rs1800562 is central for the significant changes in plasma cholesterol by altering hepatic LDLr expression in humans.

## *Hfe* deficiency increases low-density lipoprotein receptor expression and function in hepatocytes independently of iron

To examine whether iron availability impacts on HFE regulated expression of LDLr in hepatocytes, we investigated the effect of dietary iron supplementation on hepatic LDLr protein expression both in wild-type and $Hfe^{-/-}$ mice. In line with the LDL-C reduction observed in $ApoE^{-/-}Hfe^{-/-}$ mice fed an $iron^{hi}$ diet (*Figure 1C*), we found a marked increase in total hepatic LDLr protein levels in $Hfe^{-/-}$ mice on $iron^{hi}$ but not in wild-type animals fed the same diet (*Figure 4A*, Supplementary material online, *Figures S14A and B and S15A–C*). Adequate dietary iron loading was confirmed by markedly increased iron concentrations in livers of mice exposed to $iron^{hi}$ diet (*Figure 4C*), which was paralleled by increased hepatic expression of the iron storage protein ferritin (*Figure 4A*). In $Hfe^{-/-}$ mice on $iron^{hi}$ diet high intracellular iron levels were associated with increased ferritin levels and up-regulated ferroportin expression which promotes iron export from cells (*Figure 4A*).

To decipher the molecular mechanisms underlying the observed induction of the LDLr, we next performed studies using primary murine hepatocytes. In line with our reconstitution experiments, lack of *Hfe* led to increased levels of LDLr protein. Surprisingly, loading of isolated hepatocytes with holo-transferrin (holo-Tf; iron transport protein loaded with iron) did not alter LDLr protein expression any further, when compared with wild-type cells (*Figure 4B* and Supplementary material online, *Figure S16A* and *B*). Moreover, the use of the iron chelator deferiprone (DFP) to lower iron levels in our *in vitro* experiments, did not affect LDLr expression in hepatocytes. Furthermore, we did not observe differences in LDLr RNA expression between wild-type and $Hfe^{-/-}$ hepatocytes making transcriptional regulation of LDLr by Hfe unlikely. Rather, treatment of cells with the translational inhibitor cycloheximide reduced increased LDLr protein levels over time, indicating a post-/translational regulation of LDLr by Hfe (Supplementary material online, *Figure S17A–E*).

Incubation of primary hepatocytes from wild-type and $Hfe^{-/-}$ mice with BODIPY LDL-C for 1 h clearly showed enhanced LDL-C

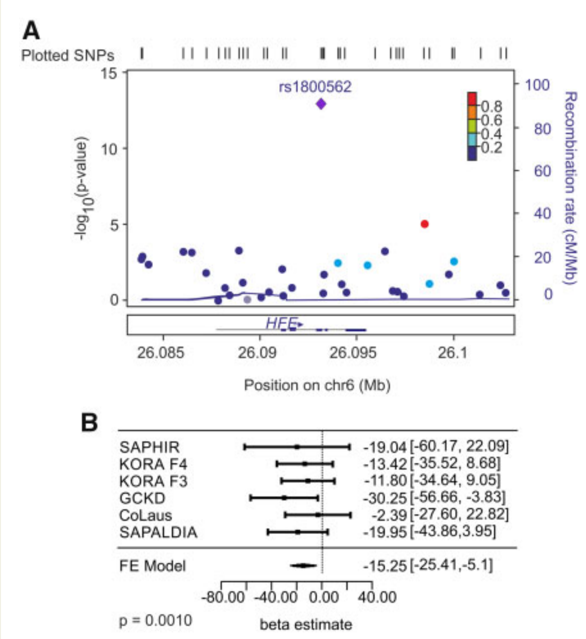


**Figure 2** Identification of HFE as regulator of LDL-C in humans. Common variants in the human *HFE* gene were evaluated in GWAS meta-analysis comprising >180 000 individuals of European ancestry. (*A*) Locus plot for LDL-C centred on the *HFE* gene. The *y*-axis reports the -$\log_{10}$ *P*-values of each SNP from Willer *et al.*[20] plotted against position on chromosome 6 using an additive genetic model; colours indicate amount of linkage disequilibrium between SNPs based on 1000 Genomes phase 3; the diamond indicates the identified lead SNP rs1800562 within *HFE*. Plot was generated using LocusZoom. (*B*) The association of the identified lead SNP rs1800562 in *HFE* with LDL-C was further analysed in six epidemiological studies using a recessive model and including a total of 24 058 individuals. Estimates are derived from a recessive coded genotype (1: AA, 0: AG/GG), adjusting for age and sex and excluding participants taking lipid-lowering drugs (Supplementary material online, *Figure S12B*). Single-study results were meta-analysed using inverse variance weighted fixed effects. The *P*-value was derived from the same model, but based on inverse normal transformed values of LDL-C to ensure normal distribution.

uptake in *Hfe*$^{-/-}$ cells compared to wild-type controls, which can be ascribed to higher LDLr expression (*Figure 4D*). To investigate cellular uptake of LDL-C at higher scrutiny, we performed time-course experiments measuring uptake of BODIPY LDL-C in primary murine hepatocytes (*Figure 4E*). Iron supplementation had no significant effect on BODIPY LDL-C uptake in either wild-type (*Figure 4F*) or *Hfe*$^{-/-}$ hepatocytes (*Figure 4G*). To rule out any non-selective and LDLr-independent uptake of LDL-C, we blocked receptor-mediated endocytosis in *Hfe*$^{-/-}$ hepatocytes by either incubating cells at 4°C, or pharmacologically using dynasore, a cell permeable, dynamin GTPase-blocking small molecule (Supplementary material online, *Figure S18A* and *B*).

To prove the pivotal role of LDLr in our model, we injected *ApoE*$^{-/-}$*Hfe*$^{-/-}$ animals with AAV8 expressing mPCSK9-D377Y ($5 \times 10^{12}$ GC per kg animal). This approach was chosen to overexpress PCSK9 in hepatocytes, and thereby silencing the hepatic LDLr (Supplementary material online, *Figure S19A* and *B*). Control littermates were injected with GFP-expressing AAV (AAV8-TBG-eGFP). Induction of a functional LDLr knockout reversed the LDL-C lowering effect observed in iron$^{hi}$-fed *ApoE*$^{-/-}$*Hfe*$^{-/-}$ animals at 3 (*Figure 4H* and *I*) *and* 9 weeks (*Figure 4J* and *K*) post-injection, respectively, confirming the central role of hepatic LDLr in Hfe-mediated control of lipid homeostasis. As shown in Supplementary material online, *Figure S20A–E*, abrogation of the cholesterol-lowering effect of iron overload in *ApoE*$^{-/-}$*Hfe*$^{-/-}$ mice also inhibited its beneficial effect on atherosclerosis. Taken together, these data demonstrate that both the hypolipidaemic as well as the anti-atherosclerotic effects observed in an animal model of haemochromatosis critically depend on hepatic LDLr expression.

## Kupffer cells are crucially involved in low-density lipoprotein cholesterol uptake *in vitro* and *in vivo*

Kupffer cell interact with hepatocytes in a paracrine manner and are involved in several metabolic processes including iron homeostasis.[16,17]

Therefore, we investigated the interplay between iron loading and regulation of cholesterol trafficking in KCs. Primary murine KCs were isolated (Supplementary material online, *Figure S21*) and subsequent immunoblot analysis showed for the first time that murine KCs express abundant amounts of LDLr (*Figure 5A*). The specificity of the employed LDLr antibody was verified using liver specimens from wild-type and *LDLr*$^{-/-}$ mice (Supplementary material online, *Figure S22*).

Immunofluorescence staining of liver sections revealed cells that are double positive for C-type lectin domain family 4, member F (Clec4f), and LDLr (*Figure 5B*), and for Clec4f and ApoB-100 (*Figure 5C*), respectively. Clec4f is a specific marker for KCs,[21] and ApoB-100 represents the main protein moiety of LDL particles, indicating a relevant uptake of LDL particles into KCs. To validate our findings on a functional level, we next performed uptake assays with BODIPY LDL-C using the immortalized murine KC cell line Kup5,[22] which displayed a KC specific antigen pattern (Supplementary material online, *Figure S23*). *Figure 5D* shows accumulation of LDL-C in intracellular granules, demonstrating efficient uptake of BODIPY LDL-C into Kup5 KCs after 24 h of incubation. Moreover, using flow cytometry, we observed a time-dependent increase of LDL-C in Kup5 cells (*Figure 5E and F*). In line with our observations made in primary KCs isolated from iron$^{hi}$ fed mice, challenge of Kup5 cells with iron led to a significant increase in mean fluorescence intensity compared to iron-depleted cells (*Figure 5E*). In addition, Kup5 cells showed an accelerated uptake of LDL-derived cholesterol due to increased expression of LDLr only if they were stimulated with iron (*Figure 5F*). Receptor-mediated endocytosis of LDL-C was completely abolished by incubating Kup5 cells at 4°C, or by using the clathrin-mediated endocytosis inhibitor dynasore (Supplementary material online, *Figure S24A* and *B*), excluding a potential non-selective uptake of LDL-C.

To estimate the ability of KCs to clear plasma LDL-C *in vivo*, we performed LDL-C turnover experiments in both wild-type and

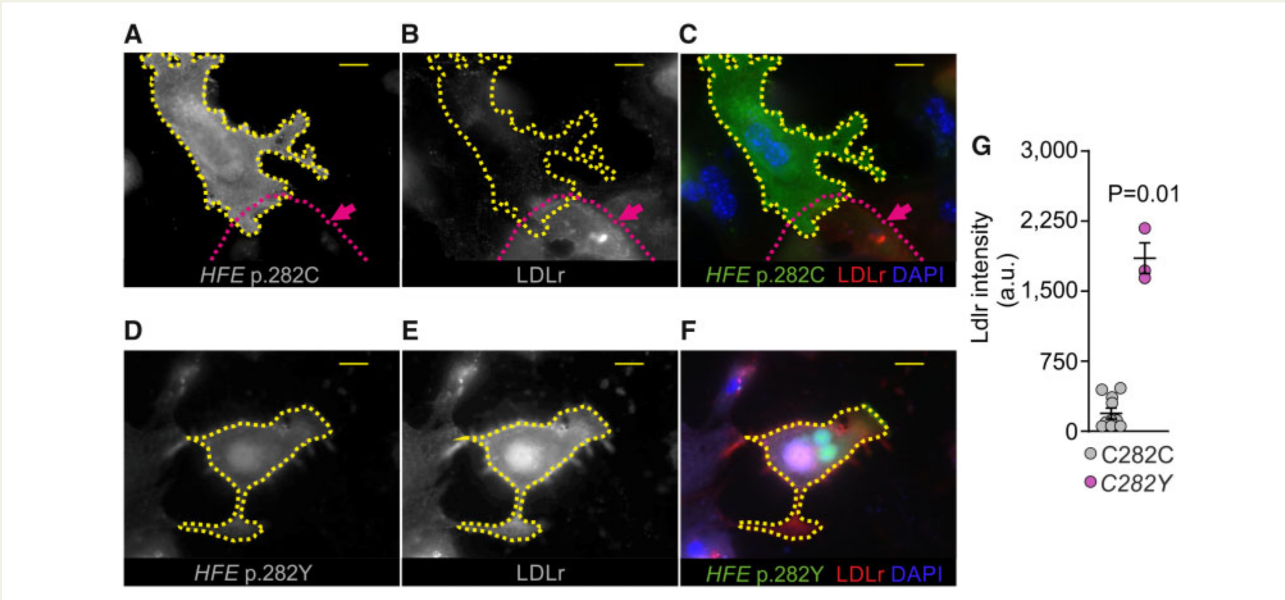


**Figure 3** Reconstitution with human HFE down-regulates LDLr expression in *Hfe*$^{-/-}$ hepatocytes. Primary murine hepatocytes isolated from *Hfe*$^{-/-}$ mice were reconstituted with wild-type HFE (*HFE* p.282C; *A–C*) or with the common human dysfunctional variant *HFE* p.282Y (*D–F*). HFE was stained with Alexa Fluor 488 (green), LDLr with Alexa Fluor 594 (red), and the nucleus was stained with DAPI (blue). Fluorescent signal is depicted in grayscale in panels (*A*), (*B*), (*D*), and (*E*); panels (*C*) and (*F*) show the combined triple staining. (*G*) Plot showing individual cell values of integrated grey scale intensity of LDLr expression ($n$ = 83 wildtype and $n$ = 56 C282Y) and means (±SEM) of 10 (wild-type *HFE* p. C282C) and 3 (*HFE* p. C282Y) experiments. Statistics was performed on the means of the individual experiments using a $t$-test assuming unequal variances ($t_{(12)}$ = -9.5, $P$ = 0.01). Scale bar = 10 µm.

*Hfe*$^{-/-}$ mice fed either an iron$^{lo}$ or iron$^{hi}$ diet, respectively. Three weeks into treatment, mice were injected with fluorescently labelled TOPFLUOR LDL-C via the tail vein. One hour after injection of labelled LDL-C, KCs were isolated by collagenase I perfusion of the liver, and subjected to flow cytometry analysis (Supplementary material online, *Figure S25*). Iron$^{hi}$ treatment led to significantly increased uptake of LDL-C in KCs, independently of the genotype, thus corroborating our results obtained in vitro (*Figure 5G*).

## Depletion of Kupffer cells leads to plasma low-density lipoprotein cholesterol accumulation

To better understand KC-dependent cholesterol transport mechanisms induced by iron loading, we performed KC depletion experiments in wild-type and *Hfe*$^{-/-}$ mice fed an iron$^{hi}$ diet for 3 weeks. For KC depletion, we used a well-established protocol[16] with intravenous injections of clodronate-containing liposomes which are phagocytosed by KCs resulting in their apoptosis (Supplementary material online, *Figure S26A*). Efficient KC depletion was ascertained by the absence of Clecf4-positive cells in the livers of clodronate-treated mice, compared to animals injected with control liposomes (Supplementary material online, *Figure S26B*). On Day 3, the time point of complete KC depletion, mice were injected with [$^3$H]-LDL-C via the tail vein. Subsequently, [$^3$H]-cholesterol levels were analysed in plasma and liver 4 h and 8 h post-injection. Notably, both *Hfe*$^{-/-}$ and wild-type mice showed significantly increased [$^3$H]-cholesterol levels in plasma upon KC depletion (Supplementary material online, *Figure S26C*), indicating accumulation of LDL-C. In contrast, no differences in liver [$^3$H]-cholesterol levels were observed, suggesting a crucial role for KCs as first-pass checkpoint for plasma LDL-C clearance and delivery to hepatocytes (Supplementary material online, *Figure S26D*).

Next, we elucidated the impact of KC mobilization on plasma LDL-C levels under dyslipidaemic conditions by studying the effect of hepatic replenishment with KCs following clodronate-mediated depletion on plasma lipoprotein metabolism in *ApoE*$^{-/-}$*Hfe*$^{-/-}$ mice on iron$^{lo/hi}$ diets (study design outlined in *Figure 5H*). Upon complete depletion of KCs (Day 3), dyslipidaemic *ApoE*$^{-/-}$*Hfe*$^{-/-}$ mice showed comparable plasma cholesterol distribution regardless of the dietary settings, i.e. iron$^{lo}$ (*Figure 5I*) or iron$^{hi}$ (*Figure 5J*). After replenishment of the hepatic niche with monocyte-derived KCs at 16 days,[21] *ApoE*$^{-/-}$*Hfe*$^{-/-}$ mice on iron$^{lo}$ diet still showed elevated LDL-C levels (*Figure 5I*), while those fed iron$^{hi}$ diet displayed a marked decrease in the LDL-C fraction compared to Day 3 (*Figure 5J*).

Together, these data identify KCs as gatekeepers for hepatic LDL-C clearance, both under physiological as well as dyslipidaemic conditions. Of note, the effect of KCs on LDL-C turnover is controlled by systemic iron availability.

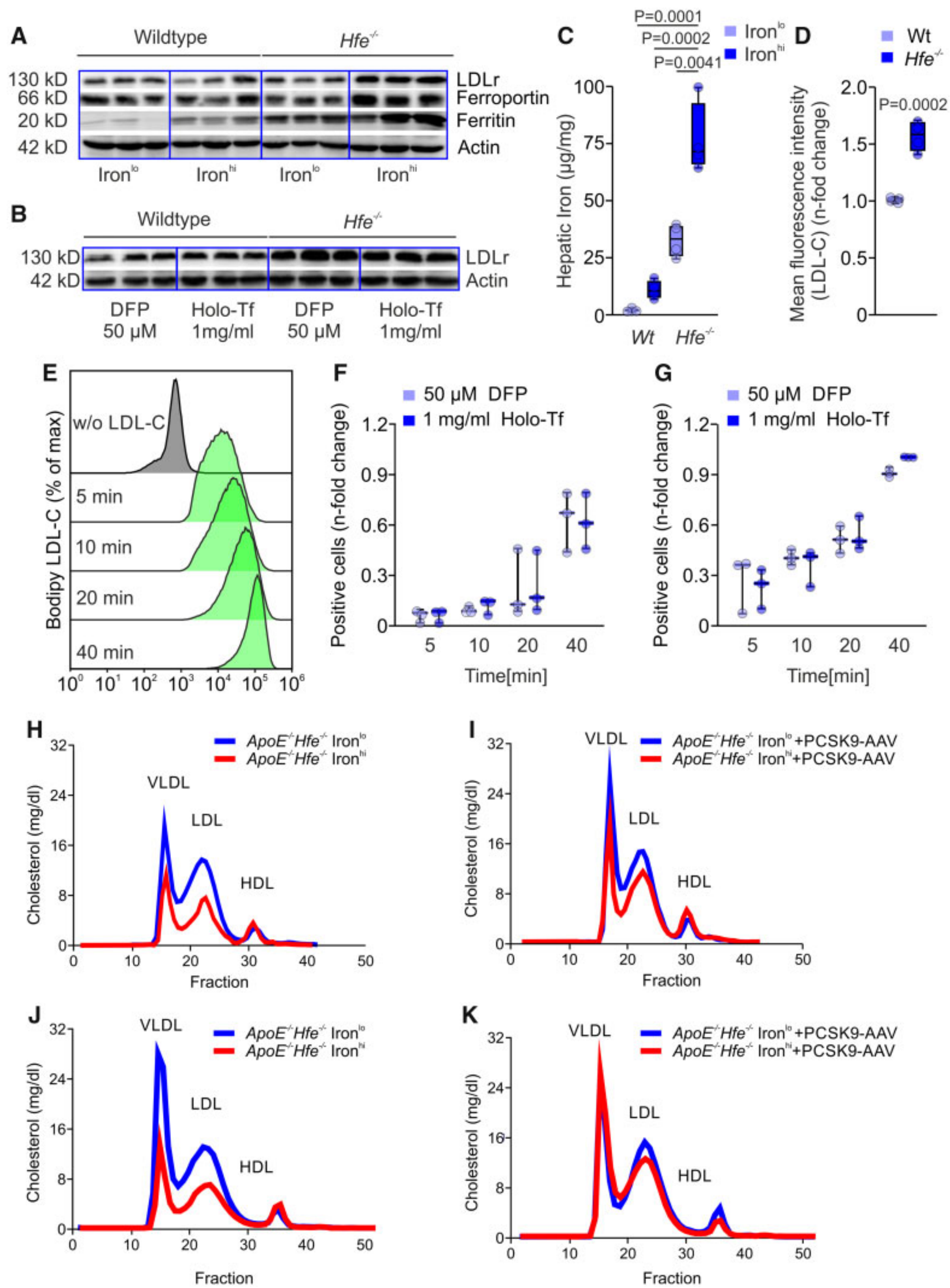


**Figure 4** Hfe affects LDLr protein expression and function in murine hepatocytes. (*A*) Immunoblot analysis of LDLr, of the iron storage protein ferritin and the iron exporter ferroportin in livers of wild-type and *Hfe*$^{-/-}$ animals fed an iron$^{lo}$ or iron$^{hi}$ diet for 3 weeks, respectively. Actin served as loading control. (*B*) Immunoblot analysis of LDLr in isolated primary murine hepatocytes of wildtype and *Hfe*$^{-/-}$ mice, incubated with the chelator deferiprone (DFP) or with 100% saturated holo-Tf for 24 h, respectively. Actin served as a loading control. (*C*) Hepatic iron measurement of wild-type and *Hfe*$^{-/-}$ animals fed iron$^{lo}$ or iron$^{hi}$ diet for 3 weeks, respectively ($n = 4$ per group). (*D*) Primary murine wild-type or *Hfe*$^{-/-}$ hepatocytes were incubated with 5 µg/mL BODIPY LDL-C for 1 h and analysed by flow cytometry ($n = 4$ per group). (*E*) Representative flow cytometry plot of primary hepatocytes incubated with BODIPY LDL-C for indicated time-points. (*F*) Primary hepatocytes isolated from wild-type and from (*G*) *Hfe*$^{-/-}$ mice were co-incubated with 5 µg/mL BODIPY LDL-C and 50 µM deferiprone (DFP) or with 1 mg/mL holo-Tf for indicated time points. LDL-C uptake was measured by flow cytometry ($n = 3$ per group). Fast protein liquid chromatography analysis of plasma pooled from *ApoE*$^{-/-}$*Hfe*$^{-/-}$ mice on western-type diet either high in iron (iron$^{hi}$) or low in iron (iron$^{lo}$) ($n = 5$ per group), at 6 weeks (*H* and *I*) and 9 weeks (*J* and *K*) after AAV-mediated knock down of LDLr via introduction of a PCSK9 overexpressing plasmid as detailed in Methods section. *ApoE*$^{-/-}$*Hfe*$^{-/-}$ mice were injected iv with AAV8-TBG-eGFP (*H* and *J*), or AAV8-mPCSK9-D377Y (*I* and *K*).

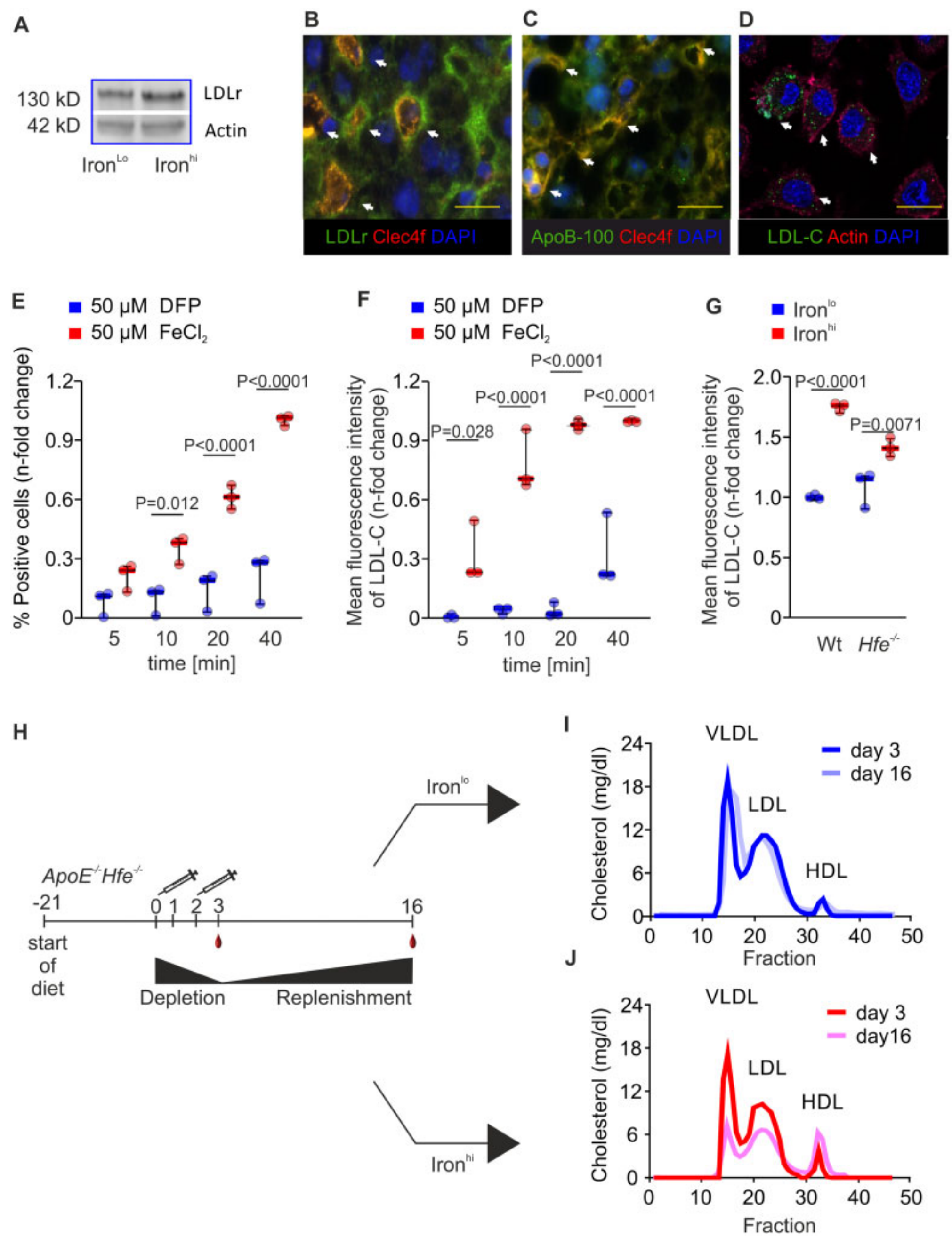


**Figure 5** KCs serve as gate-keeper for hepatic LDL-C uptake. (*A*) Immunoblot analysis of LDLr in sorted primary KCs, isolated from mice set on iron$^{lo}$ or iron$^{hi}$ diet for 3 weeks, respectively. Actin served as loading control. (*B*) Immunofluorescence staining of Clec4f and LDLr in liver sections of 8 weeks old wild-type mice (green: LDLr AF488, red: Clec4f AF594, and blue: DAPI), and (*C*) of Clec4f and ApoB-100 (green: ApoB-100 AF488, red: Clec4f AF594, and blue: DAPI). Double positive cells are marked by arrows. Scale bar = 20 μm. (*D*) Immunofluorescence staining of Kup5 cells incubated with 5 μg/mL BODIPY LDL-C for 24 h (green: BODIPY LDL-C, red: phalloidin AF594, and blue: DAPI). Kup5 cells with efficient LDL-C uptake are marked by arrows. Scale bar = 10 μm. (*E* and *F*) Kup5 cells were co-incubated with 5 μg/mL BODIPY LDL-C and 50 μM DFP or with 50 μM $FeCl_2$ for indicated time-points. (*E*) LDL-C uptake in hepatocytes was determined using flow cytometry, and given as percentage, and (*F*) mean fluorescence intensity of LDL-C positive cells ($n = 3$ per group). (*G*) Wild-type and *Hfe*$^{-/-}$ animals were fed an iron$^{lo}$ or iron$^{hi}$ diet for 3 weeks. The animals were injected with 200 μL TopFluor LDL-C (1 mg/mL) via the tail vein. One hour after injection of labelled LDL-C, KCs were isolated and mean fluorescent intensity of TopFluor LDL-C in KCs was measured with flow cytometry ($n = 3$ per group). (*H*) Replenishment of the hepatic KC pool after depletion lowers LDL-C in iron$^{hi}$ fed double knockout mice. *ApoE*$^{-/-}$*Hfe*$^{-/-}$ mice were fed an iron$^{hi}$ or iron$^{lo}$ diet for 3 weeks, respectively. Animals were then injected iv with 200 μL clodronate-containing liposomes at Day 0 and 2. Fast protein liquid chromatography analysis of pooled plasma of iron$^{lo}$ (*I*) and iron$^{hi}$ (*J*) fed *ApoE*$^{-/-}$*Hfe*$^{-/-}$ mice was performed on the day of complete KC depletion, i.e. Day 3, and on day of the replenishment of the hepatic KC pool, i.e. day 16 ($n = 4$–6 per group).

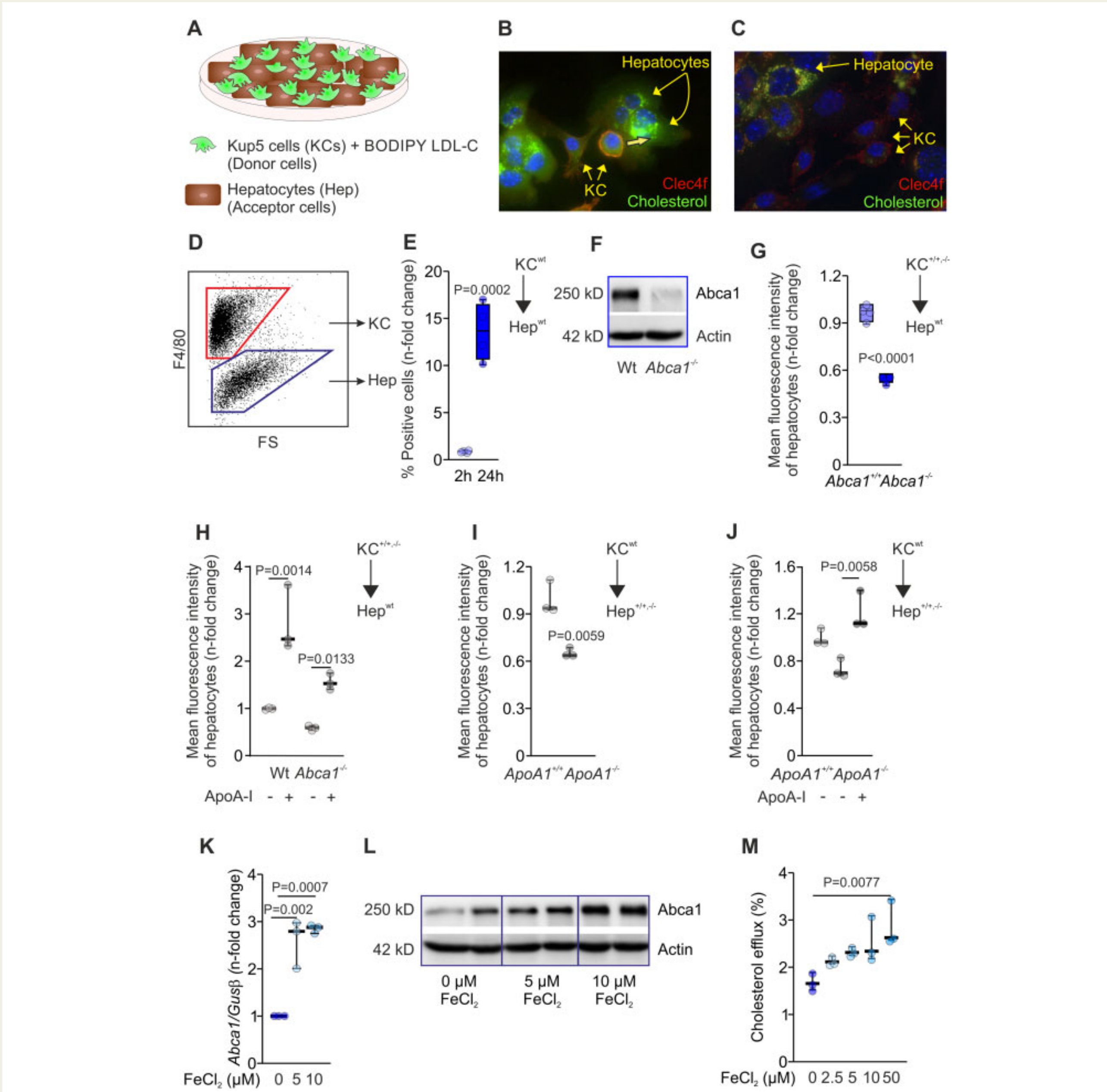


**Figure 6** KCs mediate transflux of cholesterol to hepatocytes. (*A*) Kup5 cells were loaded with 5 μg/mL BODIPY LDL-C for 24 h. Subsequently, cholesterol loaded Kup5 cells were co-incubated with primary murine hepatocytes for another 24 h. (*B* and *C*) Immunofluorescence staining of co-culture after (*B*) 24 h and (*C*) 48 h (red: Clec4f AF594, green: BODIPY LDL, and blue: DAPI). Positive cells are marked by arrows. (*D*) Representative flow cytometry plot of co-cultured cells after 24 h. Cell types were discriminated using F4/80 as specific marker for liver-resident macrophages, i.e. KCs. (*E*) LDL-C transfer from Kup5 cells to hepatocytes after 2 h and 24 h of co-culture was measured using flow cytometry. Values are depicted as median with interquartile range (boxes), whiskers represent 1.5× IRQ. Two-way ANOVA ($n = 4$ per group) (unpaired Student's *t*-test; two-tailed). (*F*) Genetic knockout of the cholesterol efflux pump Abca1 in Kup5 cells using the CRISPR/Cas9 technology was verified by immunoblot analysis. Actin served as loading control. (*G*) BODIPY LDL-C transfer from $Abca1^{+/+}$ and $Abca1^{-/-}$ Kup5 cells to primary murine hepatocytes after 24 h of co-culture was measured using flow cytometry ($n = 4$ per group). (*H*) BODIPY LDL-C transfer from $Abca1^{+/+}$ and $Abca1^{-/-}$ Kup5 cells to primary murine hepatocytes in the presence of 10 μg/mL recombinant ApoA-I was measured after 24 h of co-culture using flow cytometry ($n = 3$ per group). (*I*) BODIPY LDL-C transfer from wild-type Kup5 cells to primary murine hepatocytes derived from $ApoA1^{-/-}$ or wild-type littermates after 24 h of co-culture was measured using flow cytometry ($n = 3$ per group). (*J*) BODIPY LDL-C transfer from wild-type Kup5 cells to primary murine hepatocytes derived from $ApoA1^{-/-}$ or wild-type littermates incubated with 10 μg/mL recombinant ApoA-I after 24 h of co-culture was measured using flow cytometry ($n = 3$ per group). (*K*) qRT-PCR analysis of *Abca1* in Kup5 cells treated with indicated concentrations of $FeCl_2$ for 24 h. (*L*) Immunoblot analysis of Abca1 expression in Kup5 cells treated with indicated concentrations of $FeCl_2$ for 24 h. Actin served as loading control ($n = 3$ per group). (*M*) Cholesterol efflux of Kup5 cells to 10 μg/mL recombinant ApoA-I treated with increasing concentrations of $FeCl_2$ ($n = 3$ per group).

### Kupffer cells transfer cholesterol to hepatocytes in an Abca1-dependent fashion

To investigate the mechanisms by which KCs transfer plasma-derived LDL-C to hepatocytes, we performed co-culture experiments. To mimic first-pass clearance of plasma LDL-C by KCs, Kup5 cells were loaded with BODIPY LDL-C and subsequently co-cultured with primary murine hepatocytes (*Figure 6A*). Kupffer cells gradually transferred BODIPY cholesterol to hepatocytes over time, emptying their LDL-C cargo at 48 h of co-culture (*Figure 6B* and *C*), which is indicative of an unidirectional transport of excess cholesterol from KCs to hepatocytes over time. This finding was corroborated by flow cytometry experiments showing that hepatocytes accumulate cholesterol originating from KCs in a time-dependent manner (*Figure 6D and E*).

Cholesterol accumulation induces LXR-dependent transcription of ATP-binding cassette 1 (Abca1) in macrophages, leading to unidirectional efflux of cholesterol to ApoA-I particles, which are released into circulation by the liver.[14,23] Assuming analogous mechanisms to prevent cholesterol accumulation in KCs, we performed a series of co-culture experiments using *Abca1*$^{-/-}$ Kup5 cells and primary murine hepatocytes. Genetic knockout of *Abca1* in Kup5 cells was achieved by CRISPR/Cas9 technology (*Figure 6F*). Accordingly, hepatocyte-directed efflux of LDL-derived BODIPY cholesterol was significantly reduced in *Abca1*$^{-/-}$ and in *Abcg1*$^{-/-}$ KCs (*Figure 6G* and Supplementary material online, *Figure S27A–C*). Because Abca1-mediated cholesterol efflux needs ApoA-I as extracellular acceptor we investigated hepatocyte-directed transfer of BODIPY cholesterol in wild-type and *Abca1*$^{-/-}$ KCs incubated with recombinant ApoA-I. Addition of ApoA-I drastically increased KC-to-hepatocyte cholesterol transflux in wild-type Kup5 cells, while it had only modest effects in *Abca1*$^{-/-}$ Kup5 cells, indicative of a dysfunctional Abca1-mediated efflux mechanism (*Figure 6H*). Moreover, when measuring transfer of BODIPY cholesterol from Kup5 cells to hepatocytes lacking ApoA-I synthesis and secretion, i.e. primary murine *Apoa1*$^{-/-}$ hepatocytes, cholesterol transfer was significantly decreased (*Figure 6I*), while it was restored by addition of recombinant ApoA-I (*Figure 6J*).

In our experiments with iron$^{hi}$ treated mice, enhanced LDL-C clearance was traced back to increased LDLr expression in KCs. Accumulating intracellular cholesterol, in turn is thought to induce the expression of Abca1 in KCs, promoting the transfer of cholesterol to hepatocytes. However, we wondered whether iron supplementation *per se* might have regulatory effects on Abca1 expression in KCs, thereby accelerating the disposal of LDL-derived cholesterol in mice. As shown in *Figure 6K and L*, incubation of Kup5 cells with increasing doses of iron induced both, mRNA and protein expression of *Abca1* in this murine KC line, thus leading to an enhanced ApoA-I directed cholesterol efflux (*Figure 6M*).

# Discussion

Hereditary haemochromatosis is one of the most frequent autosomal recessive diseases in people of European origin mostly originating from a loss-of-function mutation of *HFE*(C282Y), which results in parenchymal accumulation of excess iron over time and subsequent tissue damage.[7–9,11] Importantly, a recently published UK Biobank study involving more than 400 000 European subjects including individuals with homozygous C282Y mutation reported that *HFE* deficiency was associated with a lower prevalence of coronary artery disease.[10]

In a systematic approach implementing GWAS analyses in humans and mechanistic studies in cells and mice, we were able to identify novel pathways that link HFE, iron and KC biology to the control of cholesterol homeostasis and which provide a mechanistic explanation for the lower prevalence of cardiovascular disease in HH subjects.

Using a mouse model of dyslipidaemia and HH, we found that *Hfe* deficiency protects from the development of atherosclerosis in a setting of overt iron overload. Mechanistically, we unravelled two atheroprotective mechanisms: first, iron overload leads to increased plasma clearance of LDL-C by liver-resident KCs and promotes its subsequent transfer to hepatocytes via Abca1; second, lack of Hfe leads to increased LDLr expression in hepatocytes, further accelerating LDL-C clearance. We confirmed this finding in humans by showing that *HFE* SNPs associate with LDL-C in human plasma in the GLGC dataset, to our knowledge, the largest genetic dataset on quantitative lipid traits. Importantly, these findings were replicated by performing an independent meta-analysis of six epidemiological studies containing >24 000 individuals using a recessive model. Moreover, the results also confirmed the previously published ARIC and HEIRS trials, which made the observation that individuals carrying the C282Y mutation of the *HFE* gene showed lower LDL-C levels than subjects carrying wild-type alleles.[24,25]

Mechanistically, we show that HFE acts as repressor of LDLr expression, and that HFE depletion or non-functional C282Y mutated *HFE* translate into markedly increased LDLr levels on hepatocytes. Moreover, by inducing a functional knockdown of LDLr through AAV-mediated hepatic overexpression of PCSK9, the effects of Hfe on lipoprotein profiles were completely abolished in mice.

In summary, we prove that HFE controls LDL-C serum levels by affecting LDLr expression in hepatocytes. HFE-mediated regulation of hepatocyte LDLr was not affected by iron challenge, neither *in vivo* nor *in vitro*. This indicated that iron loading exerts its effects on lipid homeostasis by a different mechanism. Investigating the underlying mechanism, we found that KCs are centrally involved in transcellular fluxes of cholesterol and that this pathway is regulated by iron availability.

Here, we identified KCs to be pivotal for hepatic LDL-C clearance, an idea that has already been addressed in experiments employing injections of [$^{125}$I]-LDL in rabbits.[26,27] Noteworthy, Nenseter *et al.*[27] showed that non-parenchymal hepatic cells including KCs may account for up to 30% of all radioactivity found in liver of hypercholesterolaemic rabbits, as compared to 6% in normolipidemic rabbits. In addition, iron overload led to decreased LDL-C levels in plasma of hypercholesterolaemic rats.[28] Together, the aforementioned studies were mainly descriptive, but confirming the mechanisms described herein by us.

Corroborating the physiological importance of KCs as temporary LDL-C storage prior to its disposal via hepatocytes, depletion of KCs caused a dramatic accumulation of LDL-C in plasma. Interestingly, dietary supplementation of KC-depleted mice with high iron concentrations led to a normalization of plasma LDL-C levels, which could

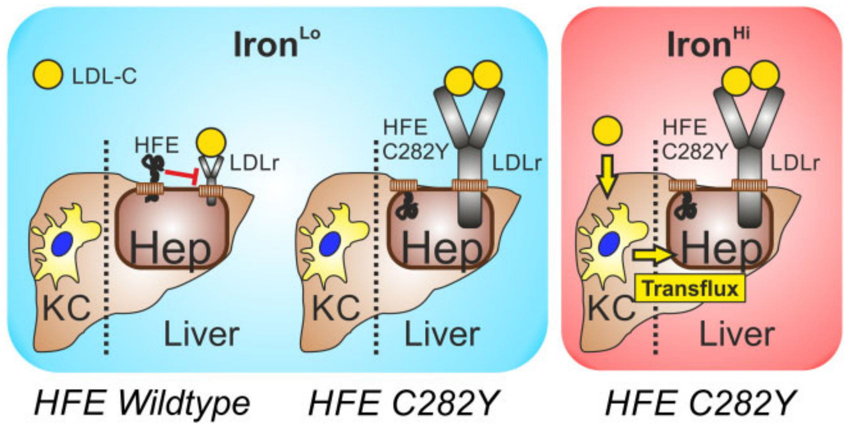


**Take home figure** HFE acts as repressor of LDLr expression: non-functional C282Y mutated HFE leads to markedly increased LDLr expression on hepatocytes and therefore to an enhanced clearance of LDL-C from circulation, when compared with a functional HFE. In addition, iron overload leads to increased plasma clearance of LDL-C by liver-resident Kupffer cells and promotes its subsequent transflux to hepatocytes.

be traced back to iron-dependent induction of trans-cellular cholesterol flux in KCs via (i) increased LDLr expression and function, and (ii) increased Abca1-mediated and ApoA-I-dependent transfer of cholesterol to hepatocytes. So far, Abca1/ApoA-I dependent cholesterol efflux was known to take place in atherosclerotic plaque macrophages upon intracellular cholesterol accumulation,[29] but it was not known that analogous mechanisms take place under physiological conditions in KCs. Moreover, the anatomical proximity of the main source of ApoA-I synthesis, i.e. hepatocytes, to KCs suggests the existence of such an important cell–cell interaction. Along this line, the over-expression of cholesteryl ester transfer protein in KCs was associated with a modulation of lipoprotein profiles towards a pro-atherogenic phenotype in mice.[30,31]

Recent data employing a mouse model with a mutation in the iron export protein ferroportin (*C326S*) described a progression of atherosclerosis linked to toxic iron accumulation in vascular tissue, inflammation and cellular apoptosis.[32] This is in line with the effects of excess non-transferrin bound iron as a catalyst for toxic radical formation.[33] Of note, this mouse model (*C326S*) differs in several aspects from the haemochromatosis model ($Hfe^{-/-}$) used in our study, at least due to the fact that the *C326S* mutation causes macrophage iron accumulation[34] whereas $Hfe^{-/-}$ mice and *C282Y* humans are characterized by macrophage iron deficiency.[35,36] However, both studies confirm the critical role of iron homeostasis for atherosclerosis development either by directly causing inflammation[32] or by modifying lipid homeostasis as shown herein. Of interest, we found no differences in systemic inflammatory status and in macrophage polarization between $ApoE^{-/-}Hfe^{-/-}$ mice on iron$^{lo/hi}$ diet. However, iron loading resulted in altered lymphocyte gene signature within the lesions of animals after 10 weeks. Whether this is a direct consequence of iron levels—given that iron can impact on lymphocyte differentiation[37]—or whether it just reflects a reduced atherosclerotic burden as a consequence of reduced cholesterol deposition in mice receiving a iron$^{hi}$ diet remains to be elucidated. However, our experiments employing PCSK9-mediated depletion of hepatic LDLr (Supplementary material online, *Figure S19A and B*) unequivocally show cholesterol lowering to be a main anti-atherosclerotic mechanism of HFE.

To summarize, we uncovered novel clinically relevant mechanisms by which dietary and genetic modulation of iron metabolism as well as KCs impact on circulating LDL-C levels in humans and mice (*Take home figure*). Our study indicates HFE and KCs as a promising target to reduce plasma LDL-C and to treat atherosclerosis.

# Supplementary material

Supplementary material is available at *European Heart Journal* online.

## Acknowledgements

The authors sincerely thank Christoph Mader and Paul Höller for excellent technical support.

## Funding

This work was supported by the Austrian Science Fund (FWF), FWF project [TRP-188] (to G.W.), Doctoral program HOROS [W-1253] (to G.W. C.V., V.P., S.D., F.K., and M.B.-P.), the Christian Doppler Society (to G.W.), and by the intramural funding programme of the Medical University Innsbruck for young scientists MUI-START, Project [2017-01-011] (to E.D.). S.K., J.W., G.W., and I.T. are supported by COMET project VASCage Tyrol [K-Project No. 843536] of the Austrian Research Promotion Agency FFG. SAPALDIA was funded by the Swiss National Science Foundation [33CS30-148470/1&2] (to N.M.P.-H.).

**Conflict of interest:** none declared.

## References

1. Ference BA, Ginsberg HN, Graham I, Ray KK, Packard CJ, Bruckert E, Hegele RA, Krauss RM, Raal FJ, Schunkert H, Watts GF, Borén J, Fazio S, Horton JD, Masana L, Nicholls SJ, Nordestgaard BG, van de Sluis B, Taskinen M-R, Tokgözoğlu L, Landmesser U, Laufs U, Wiklund O, Stock JK, Chapman MJ, Catapano AL. Low-density lipoproteins cause atherosclerotic cardiovascular disease. 1. Evidence from genetic, epidemiologic, and clinical studies. A consensus statement from the European Atherosclerosis Society Consensus Panel. *Eur Heart J* 2017;**38**:2459–2472.

2. Tall AR, Yvan-Charvet L. Cholesterol, inflammation and innate immunity. *Nat Rev Immunol* 2015;**15**:104–116.
3. Swirski FK, Nahrendorf M, Libby P. Mechanisms of myeloid cell modulation of atherosclerosis. *Microbiol Spectr* 2016;**4**.
4. Sullivan JL. Macrophage iron, hepcidin, and atherosclerotic plaque stability. *Exp Biol Med (Maywood)* 2007;**232**:1014–1020.
5. Ellervik C, Birgens H, Tybjaerg-Hansen A, Nordestgaard BG. Hemochromatosis genotypes and risk of 31 disease endpoints: meta-analyses including 66,000 cases and 226,000 controls. *Hepatology* 2007;**46**:1071–1080.
6. Feder JN, Gnirke A, Thomas W, Tsuchihashi Z, Ruddy DA, Basava A, Dormishian F, Domingo R, Ellis MC, Fullan A, Hinton LM, Jones NL, Kimmel BE, Kronmal GS, Lauer P, Lee VK, Loeb DB, Mapa FA, McClelland E, Meyer NC, Mintier GA, Moeller N, Moore T, Morikang E, Prass CE, Quintana L, Starnes SM, Schatzman RC, Brunke KJ, Drayna DT, Risch NJ, Bacon BR, Wolff RK. A novel MHC class I-like gene is mutated in patients with hereditary haemochromatosis. *Nat Genet* 1996;**13**:399–408.
7. Brissot P, Pietrangelo A, Adams PC, de Graaff B, McLaren CE, Loréal O. Haemochromatosis. *Nat Rev Dis Primers* 2018;**4**:18016.
8. Anderson GJ, Ramm GA, Subramaniam VN, Powell LW. HFE gene and hemochromatosis. *J Gastroenterol Hepatol* 2004;**19**:712–712.
9. Weiss G. Genetic mechanisms and modifying factors in hereditary hemochromatosis. *Nat Rev Gastroenterol Hepatol* 2010;**7**:50–58.
10. Pilling LC, Tamosauskaite J, Jones G, Wood AR, Jones L, Kuo CL, Kuchel GA, Ferrucci L, Melzer D. Common conditions associated with hereditary haemochromatosis genetic variants: cohort study in UK Biobank. *BMJ* 2019;**364**:k5222.
11. Adams PC, Pankow JS, Barton JC, Acton RT, Leiendecker-Foster C, McLaren GD, Speechley M, Eckfeldt JH. HFE C282Y homozygosity is associated with lower total and low-density lipoprotein cholesterol: the Hemochromatosis and Iron Overload Screening Study. *Circ Cardiovasc Genet* 2009;**2**:34–37.
12. Tuomainen TP, Kontula K, NyyssöNen K, Lakka TA, Heliö T, Salonen JT, Increased risk of acute myocardial infarction in carriers of the hemochromatosis gene Cys282Tyr mutation: a Prospective Cohort Study in Men in Eastern Finland. *Circulation* 1999;**100**:1274–1279.
13. Muckenthaler MU, Rivella S, Hentze MW, Galy B. A red carpet for iron metabolism. *Cell* 2017;**168**:344–361.
14. Rader DJ. Molecular regulation of HDL metabolism and function: implications for novel therapies. *J Clin Invest* 2006;**116**:3090–3100.
15. Gomez Perdiguero E, Klapproth K, Schulz C, Busch K, Azzoni E, Crozet L, Garner H, Trouillet C, de Bruijn MF, Geissmann F, Rodewald HR. Tissue-resident macrophages originate from yolk-sac-derived erythro-myeloid progenitors. *Nature* 2015;**518**:547–551.
16. Demetz E, Schroll A, Auer K, Heim C, Patsch JR, Eller P, Theurl M, Theurl I, Theurl M, Seifert M, Lener D, Stanzl U, Haschka D, Asshoff M, Dichtl S, Nairz M, Huber E, Stadlinger M, Moschen AR, Li X, Pallweber P, Scharnagl H, Stojakovic T, März W, Kleber ME, Garlaschelli K, Uboldi P, Catapano AL, Stellaard F, Rudling M, Kuba K, Imai Y, Arita M, Schuetz JD, Pramstaller PP, Tietge UJF, Trauner M, Norata GD, Claudel T, Hicks AA, Weiss G, Tancevski I. The arachidonic acid metabolome serves as a conserved regulator of cholesterol metabolism. *Cell Metab* 2014;**20**:787–798.
17. Theurl I, Hilgendorf I, Nairz M, Tymoszuk P, Haschka D, Asshoff M, He S, Gerhardt LMS, Holderried TAW, Seifert M, Sopper S, Fenn AM, Anzai A, Rattik S, McAlpine C, Theurl M, Wieghofer P, Iwamoto Y, Weber GF, Harder NK, Chousterman BG, Arvedson TL, McKee M, Wang F, Lutz OM, Rezoagli E, Babitt JL, Berra L, Prinz M, Nahrendorf M, Weiss G, Weissleder R, Lin HY, Swirski FK. On-demand erythrocyte disposal and iron recycling requires transient macrophages in the liver. *Nat Med* 2016;**22**:945–951.
18. Maia ML, Pereira CS, Melo G, Pinheiro I, Exley MA, Porto G, Macedo MF. Invariant natural killer T cells are reduced in hereditary hemochromatosis patients. *J Clin Immunol* 2015;**35**:68–74.
19. Han ES, Muller FL, Pérez VI, Qi W, Liang H, Xi L, Fu C, Doyle E, Hickey M, Cornell J, Epstein CJ, Roberts LJ, Van Remmen H, Richardson A. The in vivo gene expression signature of oxidative stress. *Physiol Genomics* 2008;**34**:112–126.
20. Willer CJ, Schmidt EM, Sengupta S, Peloso GM, Gustafsson S, Kanoni S, Ganna A, Chen J, Buchkovich ML, Mora S, Beckmann JS, Bragg-Gresham JL, Chang H-Y, Demirkan A, Den Hertog HM, Do R, Donnelly LA, Ehret GB, Esko T, Feitosa MF, Ferreira T, Fischer K, Fontanillas P, Fraser RM, Freitag DF, Gurdasani D, Heikkilä K, Hyppönen E, Isaacs A, Jackson AU, Johansson Å, Johnson T, Kaakinen M, Kettunen J, Kleber ME, Li X, Luan J, Lyytikäinen L-P, Magnusson PKE, Mangino M, Mihailov E, Montasser ME, Müller-Nurasyid M, Nolte IM, O'Connell JR, Palmer CD, Perola M, Petersen A-K, Sanna S, Saxena R, Service SK, Shah S, Shungin D, Sidore C, Song C, Strawbridge RJ, Surakka I, Tanaka T, Teslovich TM, Thorleifsson G, Van den Herik EG, Voight BF, Volcik KA, Waite LL, Wong A, Wu Y, Zhang W, Absher D, Asiki G, Barroso I, Been LF, Bolton JL, Bonnycastle LL, Brambilla P, Burnett MS, Cesana G, Dimitriou M, Doney ASF, Döring A, Elliott P, Epstein SE, Ingi Eyjolfsson G, Gigante B, Goodarzi MO, Grallert H, Gravito ML, Groves CJ, Hallmans G, Hartikainen A-L, Hayward C, Hernandez D, Hicks AA, Holm H, Hung Y-J, Illig T, Jones MR, Kaleebu P, Kastelein JJP, Khaw K-T, Kim E, Klopp N, Komulainen P, Kumari M, Langenberg C, Lehtimäki T, Lin S-Y, Lindström J, Loos RJF, Mach F, McArdle WL, Meisinger C, Mitchell BD, Müller G, Nagaraja R, Narisu N, Nieminen TVM, Nsubuga RN, Olafsson I, Ong KK, Palotie A, Papamarkou T, Pomilla C, Pouta A, Rader DJ, Reilly MP, Ridker PM, Rivadeneira F, Rudan I, Ruokonen A, Samani N, Scharnagl H, Seeley J, Silander K, Stančáková A, Stirrups K, Swift AJ, Tiret L, Uitterlinden AG, van Pelt LJ, Vedantam S, Wainwright N, Wijmenga C, Wild SH, Willemsen G, Wilsgaard T, Wilson JF, Young EH, Zhao JH, Adair LS, Arveiler D, Assimes TL, Bandinelli S, Bennett F, Bochud M, Boehm BO, Boomsma DI, Borecki IB, Bornstein SR, Bovet P, Burnier M, Campbell H, Chakravarti A, Chambers JC, Chen Y-DI, Collins FS, Cooper RS, Danesh J, Dedoussis G, de Faire U, Feranil AB, Ferrières J, Ferrucci L, Freimer NB, Gieger C, Groop LC, Gudnason V, Gyllensten U, Hamsten A, Harris TB, Hingorani A, Hirschhorn JN, Hofman A, Hovingh GK, Hsiung CA, Humphries SE, Hunt SC, Hveem K, Iribarren C, Järvelin M-R, Jula A, Kähönen M, Kaprio J, Kesäniemi A, Kivimaki M, Kooner JS, Koudstaal PJ, Krauss RM, Kuh D, Kuusisto J, Kyvik KO, Laakso M, Lakka TA, Lind L, Lindgren CM, Martin NG, März W, McCarthy MI, McKenzie CA, Meneton P, Metspalu A, Moilanen L, Morris AD, Munroe PB, Njølstad I, Pedersen NL, Power C, Pramstaller PP, Price JF, Psaty BM, Quertermous T, Rauramaa R, Saleheen D, Salomaa V, Sanghera DK, Saramies J, Schwarz PEH, Sheu WH-H, Shuldiner AR, Siegbahn A, Spector TD, Stefansson K, Strachan DP, Tayo BO, Tremoli E, Tuomilehto J, Uusitupa M, van Duijn CM, Vollenweider P, Wallentin L, Wareham NJ, Whitfield JB, Wolffenbuttel BHR, Ordovas JM, Boerwinkle E, Palmer CNA, Thorsteinsdottir U, Chasman DI, Rotter JI, Franks PW, Ripatti S, Cupples LA, Sandhu MS, Rich SS, Boehnke M, Deloukas P, Kathiresan S, Mohlke KL, Ingelsson E, Abecasis GR; Global Lipids Genetics Consortium. Discovery and refinement of loci associated with lipid levels. *Nat Genet* 2013;**45**:1274–1283.
21. Scott CL, Zheng F, De Baetselier P, Martens L, Saeys Y, De Prijck S, Lippens S, Abels C, Schoonooghe S, Raes G, Devoogdt N, Lambrecht BN, Beschin A, Guilliams M. Bone marrow-derived monocytes give rise to self-renewing and fully differentiated Kupffer cells. *Nat Commun* 2016;**7**:10321.
22. Kitani H, Sakuma C, Takenouchi T, Sato M, Yoshioka M, Yamanaka N. Establishment of c-myc-immortalized Kupffer cell line from a C57BL/6 mouse strain. *Results Immunol* 2014;**4**:68–74.
23. Ye D, Lammers B, Zhao Y, Meurs I, Van Berkel TJ, Van Eck M. ATP-binding cassette transporters A1 and G1, HDL metabolism, cholesterol efflux, and inflammation: important targets for the treatment of atherosclerosis. *Curr Drug Targets* 2011;**12**:647–660.
24. Pankow JS, Boerwinkle E, Adams PC, Guallar E, Leiendecker-Foster C, Rogowski J, Eckfeldt JH. HFE C282Y homozygotes have reduced low-density lipoprotein cholesterol: the Atherosclerosis Risk in Communities (ARIC) study. *Transl Res* 2008;**152**:3–10.
25. Meroño T, Brites F, Dauteuille C, Lhomme M, Menafra M, Arteaga A, Castro M, Saez MS, Ballerga EG, Sorroche P, Rey J, Lesnik P, Sordá JA, Chapman MJ, Kontush A, Daruich J. Metabolic alterations, HFE gene mutations and atherogenic lipoprotein modifications in patients with primary iron overload. *Clin Sci (Lond)* 2015;**128**:609–618.
26. Kamps JA, Kruijt JK, Kuiper J, Van Berkel TJ. Uptake and degradation of human low-density lipoprotein by human liver parenchymal and Kupffer cells in culture. *Biochem J* 1991;**276**:135–140.
27. Nenseter MS, Gudmundsen O, Roos N, Maelandsmo G, Drevon CA, Berg T. Role of liver endothelial and Kupffer cells in clearing low density lipoprotein from blood in hypercholesterolemic rabbits. *J Lipid Res* 1992;**33**:867–877.
28. Turbino-Ribeiro SM, Silva ME, Chianca DA Jr, De Paula H, Cardoso LM, Colombari E, Pedrosa ML. Iron overload in hypercholesterolemic rats affects iron homeostasis and serum lipids but not blood pressure. *J Nutr* 2003;**133**: 15–20.
29. Singaraja RR, Brunham LR, Visscher H, Kastelein JJ, Hayden MR. Efflux and atherosclerosis: the clinical and biochemical impact of variations in the ABCA1 gene. *Arterioscler Thromb Vasc Biol* 2003;**23**:1322–1332.
30. Van Eck M, Ye D, Hildebrand RB, Kar Kruijt J, de Haan W, Hoekstra M, Rensen PC, Ehnholm C, Jauhiainen M, Van Berkel TJ. Important role for bone marrow-derived cholesteryl ester transfer protein in lipoprotein cholesterol redistribution and atherosclerotic lesion development in LDL receptor knockout mice. *Circ Res* 2007;**100**:678–685.
31. Wang Y, van der Tuin S, Tjeerdema N, van Dam AD, Rensen SS, Hendrikx T, Berbee JF, Atanasovska B, Fu J, Hoekstra M, Bekkering S, Riksen NP, Buurman WA, Greve JW, Hofker MH, Shiri-Sverdlov R, Meijer OC, Smit JW, Havekes LM, van Dijk KW, Rensen PC. Plasma cholesteryl ester transfer protein is predominantly derived from Kupffer cells. *Hepatology* 2015;**62**:1710–1722.

32. Vinchi F, Porto G, Simmelbauer A, Altamura S, Passos ST, Garbowski M, Silva AMN, Spaich S, Seide SE, Sparla R, Hentze MW, Muckenthaler MU. Atherosclerosis is aggravated by iron overload and ameliorated by dietary and pharmacological iron restriction. *Eur Heart J* 2019;doi:10.1093/eurheartj/ehz112.
33. Koskenkorva-Frank TS, Weiss G, Koppenol WH, Burckhardt S. The complex interplay of iron metabolism, reactive oxygen species, and reactive nitrogen species: insights into the potential of various iron therapies to induce oxidative and nitrosative stress. *Free Radic Biol Med* 2013;**65**:1174–1194.
34. Neves J, Leitz D, Kraut S, Brandenberger C, Agrawal R, Weissmann N, Mühlfeld C, Mall MA, Altamura S, Muckenthaler MU. Disruption of the hepcidin/ferroportin regulatory system causes pulmonary iron overload and restrictive lung disease. *EBioMedicine* 2017;**20**:230–239.
35. Nairz M, Theurl I, Schroll A, Theurl M, Fritsche G, Lindner E, Seifert M, Crouch ML, Hantke K, Akira S, Fang FC, Weiss G. Absence of functional Hfe protects mice from invasive Salmonella enterica serovar Typhimurium infection via induction of lipocalin-2. *Blood* 2009;**114**:3642–3651.
36. Pietrangelo A. Hereditary hemochromatosis—a new look at an old disease. *N Engl J Med* 2004;**350**:2383–2397.
37. Soares MP, Weiss G. The Iron age of host–microbe interactions. *EMBO Rep* 2015;**16**:1482–1500.